Fire Technology, 57, 1457–1478, 2021

Manufactured in The United States
https://doi.org/10.1007/s10694-020-01066-x

Improving the State-of-the-Art in Flow Measurements for Large-Scale Oxygen Consumption Calorimetry

Rodney A. Bryant and Matthew F. Bundy, Fire Research Division, National Institute of Standards and Technology, Gaithersburg, MD 20899, USA*

Received: 12 July 2020/**Accepted:** 18 November 2020

Abstract. The accuracy of the exhaust flow measurement contributes significantly to the uncertainty of calorimetry measurements for large fire testing. Less than ideal flow characteristics such as skewed velocity distributions are typical of these large-scale flows and make it difficult to achieve the desired measurement accuracy. Consensus standards for fire testing recommend either bi-directional probes or orifice plates to determine exhaust flow. Both have limited accuracy in the presence of less than ideal flow conditions. Averaging pitot probes are an off-the-shelf technology widely used to monitor flows for industrial processes. They have been utilized in a system of large fire calorimeters to demonstrate differences of less than 5% between heat release rate measurements by oxygen consumption calorimetry and the theoretical heat output from a gas burner. Differences exceeded 5% for a small set of conditions but were still less than 10%. Both levels of agreement are within the confirmation requirements of the consensus standards and were achieved without a system calibration as recommended by the standards. Including this technology as an alternate method to measure exhaust flow would be an improvement to relevant fire testing standards and to the overall accuracy of calorimetry measurements for large fire testing.

Keywords: Flow measurement, Calorimetry, Averaging pitot, Fire testing standards

List of Symbols

B	Blockage factor for averaging pitot probe
D_{eff}	Effective diameter of exhaust duct
$\left(\Delta_c H_{fuel}\right)_{O_2}$	Heat of combustion of hydrocarbon fuel per unit mass oxygen
$(\Delta_c H_{CO})_{O_2}$	Heat of combustion of carbon monoxide per unit mass oxygen
K_a	Flow coefficient for averaging pitot probe
$\dot{m}$	Mass flow
M	Molar mass
P_{amb}	Ambient pressure
ΔP	Differential pressure
$\dot{Q}_{OC}$	Rate of heat release derived from oxygen consumption (OC) calorimetry
$\dot{Q}_{FC}$	Rate of heat release derived from fuel consumption (FC) calorimetry
R	Universal gas constant

*Correspondence should be addressed to: Rodney A. Bryant, E-mail: rodney.bryant@nist.gov

Re	Reynolds number
s_i	Non-dimensional sensitivity coefficient for measurement component
T	Gas temperature
u	Standard uncertainty
U	Expanded uncertainty
x_i	Measurement component
X_i	Exhaust stream volume fraction of gas i
X_i^o	Ambient volume fraction of gas i

Greek Symbols

α	Combustion products expansion factor
ε	Estimated measurement error due to skewed velocity distribution
ρ	Gas density
σ	Standard deviation
ϕ	Oxygen depletion factor

Subscripts

e	Exhaust duct
eff	Effective
i	Gas, probe A or B

1. Introduction

The heat released from burning items is a critical measurement for large-scale fire testing. Oxygen consumption calorimetry is a widely adopted method for measuring the rate of heat release, $\dot{Q}_{OC}$, during a fire experiment or material flammability test. The computation of heat release rate, Eq. 1, requires measurements of oxygen volume fraction, X_{O_2} (where $\phi = f(X_{O_2}, X^o_{O_2}, X_{CO_2}, X^o_{CO_2}, X_{CO})$), and total gas flow, $\dot{m}_{eff}$, in the exhaust stream (flue gas) [1].

$$\dot{Q}_{OC} = \left[\left(\Delta_c H_{fuel}\right)_{O_2} \phi - \left((\Delta_c H_{CO})_{O_2} - (\Delta_c H_{fuel})_{O_2} \right) \frac{1-\phi}{2} \frac{X_{CO}}{X_{O_2}} \right] \frac{\dot{m}_{eff}}{1+\phi(\alpha-1)} \left(1 - X^o_{H_2O}\right) X^o_{O_2} \frac{M_{O_2}}{M_{air}} \tag{1}$$

Multiple studies have cited the exhaust flow measurement as a significant source of uncertainty when measuring heat release rate [2–7]. Consensus standards for open calorimetry fire testing, such as ASTM E2067, ISO 24473, and NFPA 286, recommend either a single bi-directional probe placed on centerline or an orifice plate to determine exhaust flow [8–14]. The accuracy of these measurement devices is limited when used in flows with a skewed velocity distribution. Guidance, in the form of a heat release rate or system calibration, is provided in the standards to account for error of the flow measurement. For example, when using orifice plates, the error of the heat release rate measurement and more explicitly the error of the exhaust flow measurement is inferred by comparing the known heat release from a gas burner to that measured in the exhaust flue by oxygen consumption calorimetry. The error is used to determine the flow coefficient for the orifice plate and hence apply a correction to the flow measurement (ASTM E2067, ISO 24473); or it is used to directly correct the heat release rate measurement (ASTM E1354, ASTM E2257) [8–10, 12].

ASTM E2067 and ISO 24473 offer guidance on correcting the bi-directional probe measurement to account for skewed flow by conducting a velocity traverse across the exhaust duct to determine the flow distribution. The correction is the ratio of the average velocity determined from the distribution measurements to the centerline measurement. By design, averaging pitot probes can integrate the velocity distribution and provide a single measurement representative of the average flow across the exhaust duct. Depending on the accuracy requirements for a given test method or facility, they have the potential to reduce the need for flow correction in open calorimetry measurements. Averaging pitot probes are widely used as an affordable means to monitor large-scale process flows. Relevant fire testing standards, such as those mentioned previously, should consider incorporating this technology as an alternate method to measure exhaust flow.

Averaging pitot probes (also known as flow-averaging tubes or multi-port averaging pitot tubes) are impact pressure devices that measure the differential pressure, ΔP, induced by a flowing gas or liquid. Like the standard pitot tube, Bernoulli's principle is used to infer the fluid velocity from measurements of differential pressure and fluid density, ρ. The averaging pitot probe extends across the entire diameter of the pipe and has multiple impact and static ports positioned at equal annular locations, Fig. 1. Averaging of the spatial distribution of pressure occurs inside the impact and static chambers, resulting in a differential pressure measurement that represents the mean flow velocity, V. This relationship is described in the following equation, where K_a is the flow coefficient for the averaging pitot probe.

$$V = K_a \sqrt{\frac{2\Delta P}{\rho}} \tag{2}$$

The number of impact ports and their spacing can be designed to meet specific applications, but they are usually spaced to account for a log-linear distribution of velocity [15]. The flow coefficient, K_a, ranges from 0.6 to 0.8, depending on the flow conditions and shape of the cross-section of the probe [16]. Multiple studies have investigated various probe geometries and their impact on K_a in order to optimize the performance of the device [16–19].

The National Fire Research Laboratory (NFRL), a research facility for the study of large-scale fire-structure interactions [20, 21], utilizes large fume or flue gas hoods to capture the plume of fires as large as 20 MW. The exhaust ducts that service these fume hoods can flow as much as 110 kg/s of air. The exhaust flow measurement was identified as a significant contributor to the combined uncertainty of the facility's heat release rate measurement [7]. As the facility has evolved, an effort to improve the exhaust flow measurement and reduce the measurement uncertainty has been ongoing. This effort has included increasing the straight-run of duct upstream of the flow measurement location to generate a more fully-developed flow profile and utilizing off-the-shelf technology for better flow monitoring. This has involved replacing the typical flow measurement device for fire testing—the bi-directional probe, with a state-of-the-art measurement device for industrial process flows - an averaging pitot probe. The averaging pitot probe is widely used across industries, like energy distribution and chemical production, to monitor liquid, gas, and steam pipeline flows [17].

A flow mapping study to characterize the flow distribution for an earlier configuration of NFRL's exhaust duct confirmed that skewed velocity profiles are likely in large exhaust ducts when flow conditioning is not employed [22]. The study also confirmed that the accuracy of the average flow measurement improves if measurements are made on two orthogonal chords of the exhaust duct. Following the study's recommendation, two averaging pitot probes were installed at the flow measurement stations for the exhaust system. The objectives of this study are to gain further insight into the behavior of the facility's exhaust flow system from the measured results and to demonstrate affordable and practical measurement methods for meeting the accuracy requirements of fire test standards for intermediate to large-scale calorimetry.

2. Experimental Methods and Materials

2.1. Flue Gas Exhaust System

The NFRL utilizes large-canopy exhaust hoods to capture the fire effluents for quantification of heat release as a function of time. The insulated steel hoods are suspended above the test floor and serviced by large exhaust ducts that transport the combustion products to an emissions control system (ECS) for conditioning before release into the atmosphere. The facility has 4 canopy hoods and hence 4 oxygen consumption calorimeters Fig. 2. Each calorimeter is denoted by its fire capacity, 0.5 MW, 3 MW, 10 MW, and 20 MW. Details of each calorimeter are listed in Table 1.

The 3 MW and 10 MW calorimeters are serviced by an exhaust duct with inner diameter (ID) 1.975 m. A 0.483 m ID duct feeds into the 1.975 m duct and services the 0.5 MW calorimeter. The 20 MW calorimeter is serviced by a 2.424 m ID duct. Both large ducts, 1.975 m and 2.424 m, run along the roof of the facility and transport the combustion products from the fire to the ECS, Fig. 3. Instrument measurement stations are located upstream of the ECS. At these locations, measurements of gas volume fraction, gas temperature, and gas velocity are made to determine heat release rate. The layout of the roof ducts was designed to provide more than 10 diameters of straight run to create a well-developed flow at the measurement stations. Flow is pulled through the exhaust system by induced draft fans near the end of the system. Therefore, the operating pressure in the ducts is slightly below atmospheric. The system has a mass flow capacity of approximately 110 kg/s (5100 m^3/min at standard conditions) and a heat release rate capacity of 20 MW.

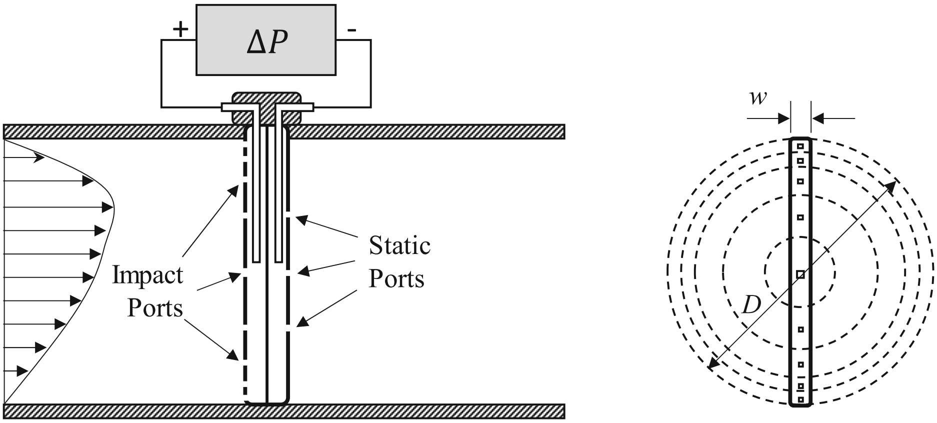

Figure 1. Generic configuration and installation for an averaging pitot probe with length D and width w. Concentric circles (dashed lines, right-most figure) are drawn to show annular locations for the impact ports.

2.2. Exhaust Flow Measurement

2.2.1. Effective Gas Velocity The flow sensors used in the exhaust ducts are tee-shaped averaging pitot style probes (Rosemont 485 Annubar)[1]. The probes are made of 316 stainless steel and have a width of 2.692 cm. Three probe lengths are used to match the inner diameter of the exhaust ducts, 0.48 m, 1.97 m and 2.42 m. Separate pairs of pitot probes (A and B), each equipped with two Type K thermocouples, are installed in the 1.975 m duct and the 2.424 m duct. The two probes are installed on orthogonal chords of the duct cross section and 45° relative to horizontal as shown in Fig. 4. At least 1 duct diameter of separation distance exists for the two-probe installation. The effective velocity at the measurement station is the average of the measurements from the two probes, A and B:

$$V_{\mathrm{eff}} = (V_{\mathrm{e,A}} + V_{\mathrm{e,B}})/2 \tag{3}$$

A single averaging pitot probe (A) and thermocouple pair are installed vertically in the 0.483 m duct for the 0.5 MW calorimeter, hence $V_{\mathrm{eff}} = V_{\mathrm{e,A}}$. The ideal installation configuration would optimize the location of the probes to provide the best accuracy. This would require a priori knowledge of the flow distribution and its stability over the range of operating conditions. Without this knowledge, the

[1] Certain commercial entities, equipment, or materials may be identified in this document in order to describe an experimental procedure or concept adequately. Such identification is not intended to imply recommendation or endorsement by the National Institute of Standards and Technology, nor is it intended to imply that the entities, materials, or equipment are necessarily the best available for the purpose.

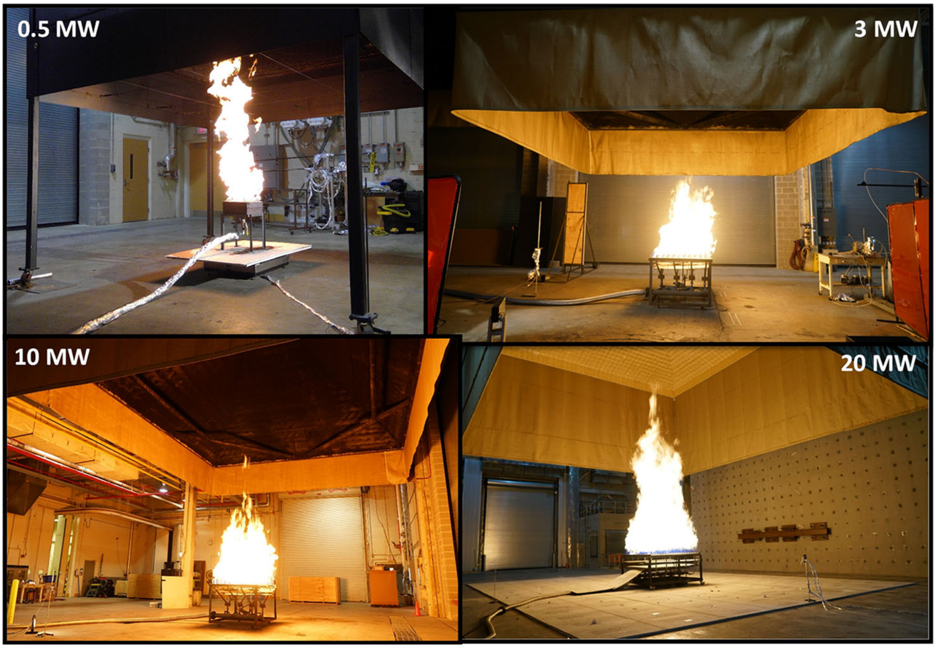

Figure 2. Photographs of the oxygen consumption calorimeters and natural gas burners.

Table 1
Characteristics of the Canopy Exhaust Hood System

Canopy hood m × m	Duct ID m	Flow capacity kg/s (m^3/min)	Fire capacity MW
3.1 × 3.2	0.483	4.1 (190)	0.5
6.1 × 6.1	1.975	27.5 (1275)	3
8.4 × 12.4	1.975	54.9 (2550)	10
13.8 × 15.4	2.424	110 (5100)	20

probes were installed on chords that provided practical convenience for installation and maintenance of the probes.

The flow-induced differential pressure, ΔP, is measured with high-precision capacitance manometers (MKS 220D Baratron). The instruments have a range of 0 Pa to 1333.2 Pa and are calibrated against an in-house working standard for pressure. The relative expanded uncertainty of the differential pressure measurement is estimated at 0.006. The measured output of each capacitance manometer is used to compute the average flow velocity, $V_{e,i}$, at each device i (i = A or B).

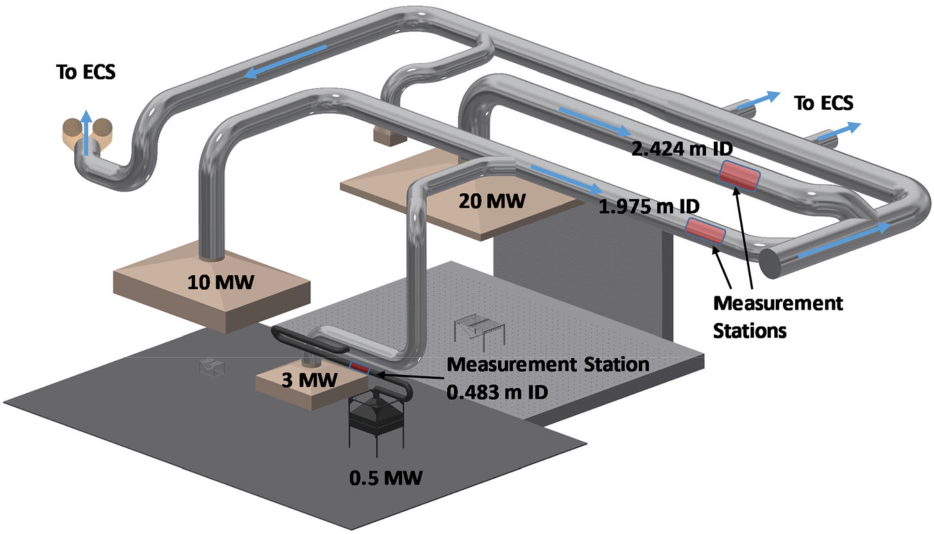

Figure 3. Digital rendering of the flue gas exhaust system. Blue arrows indicate flow direction.

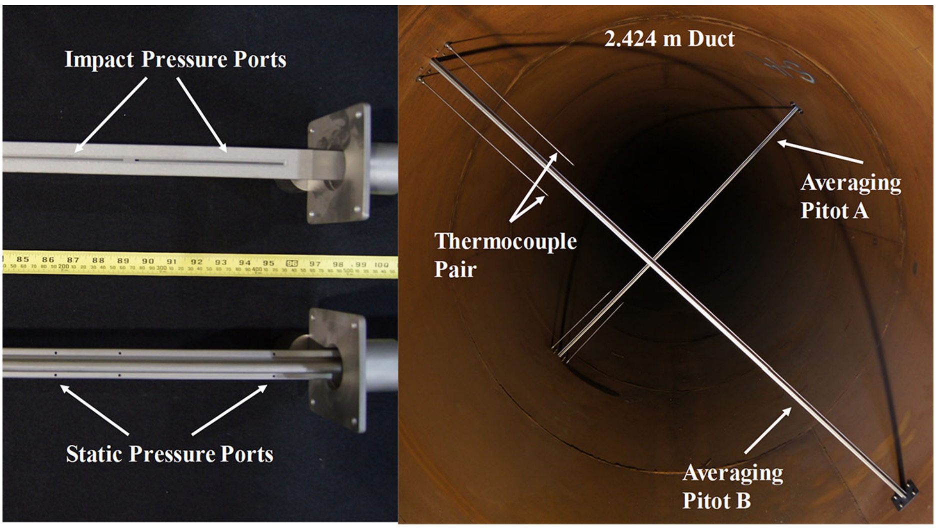

Figure 4. Installation of two averaging pitot probes in the 2.424 m exhaust duct. Photograph view is upstream and into the flow.

$$V_{e,i} = K_{a,i}\sqrt{\frac{2\Delta P_i}{\rho_{e,i}}} \tag{4}$$

The flow coefficient, K_a, for the probe was determined using the following equation from the manufacturer's reference guide [23].

$$K_a = \frac{(1 - C_2 B)}{\sqrt{1 - C_1 (1 - C_2 B)^2}} \tag{5}$$

The probe blockage factor, B, is defined as the ratio of the probe face area to the area of the duct cross section. The constants $C_1 = -1.4920$ and $C_2 = 1.4179$ are based on the probe width. Blockage factors and the resulting flow coefficients for the 3 probes are listed in Table 2. The manufacturer quotes an expanded uncertainty of 0.75% for the flow coefficients in the case of fully-developed turbulent pipe flow, therefore a flow that is symmetrical in all directions across the pipe. The uncertainty estimate is also valid when the Reynolds number (Re) for the flow over the probe is greater than 12,500. Error in the flow measurement may occur if these conditions are not met. If so, the manufacturer recommends an in-line calibration of the probe to improve measurement accuracy.

Gas density at each averaging pitot probe (i = A or B) is derived as follows:

$$\rho_{e,i} = \frac{P_{amb} M_e}{R T_{e,i}} \tag{6}$$

Each probe is equipped with two bare-bead thermocouples, type K, to provide measured estimates of gas temperature in the exhaust duct, $T_{e,A} = (T_{e,A1} + T_{e,A2})/2$ and $T_{e,B} = (T_{e,B1} + T_{e,B2})/2$. The relative expanded uncertainty for the gas temperature measurement is estimated to be 0.010. This estimate includes the relative standard uncertainty for the bead temperature as stated by the manufacturer, 0.0038, and the relative standard error due to the spatial distribution of temperature and the radiative heat transfer with the surroundings, 0.0035. Both were combined in quadrature. To get a preliminary scope of the temperature distribution, two bare-bead thermocouples were temporarily placed in other portions of the exhaust flow in addition to the four thermocouples attached to the averaging pitot probes. The maximum difference in thermocouple readings was less 0.6% for 6 different locations and 6 different thermocouples. Assuming a rectangular distribution of uncertainty due to this range of measurements, the difference was used to estimate the relative standard error due to temperature distribution and radiation, $0.0035 = 0.006/\sqrt{3}$. Practical approaches such as this are recommended to estimate the temperature distribution and its impact on mass flow measurements.

The ambient pressure, P_{amb}, inside the facility is measured with a digital barometer (Vaisala PTB220) with an expanded uncertainty of 103 Pa. The molar mass, M_e, of the exhaust gas is assumed to be equal to that of the dry ambient air,

Table 2
Characterizing Details for the Averaging Pitot Probes. Expanded Uncertainties are Reported for a 95% Confidence Interval with a Coverage Factor k = 2.0

Probe length, m	B	K_a	Calorimeter
0.48	0.0707	0.6055 ± 0.0045	0.5 MW
1.97	0.0174	0.6271 ± 0.0047	3 MW
			10 MW
2.42	0.0141	0.6283 ± 0.0047	20 MW

28.97 ± 0.10 kg/kmole. This assumption is applied since the exhaust ducts are designed to pull significantly more air than required for complete combustion and the combustion products of the fire are only a small contribution to the total mass of the exhaust gases.

2.2.2. Effective Duct Diameter The cross-sectional area of the duct is determined based on its effective diameter, D_{eff}, for flow analysis (hydraulic diameter). It is defined as the diameter of a circle with the same cross-sectional area as the nearly circular duct. The effective diameter was determined as the average length of the measured chords at the two planes containing the averaging pitot probes. Effective duct diameters along with their expanded uncertainty estimates are listed in Table 3. The uncertainty estimates account for the standard error of the mean and the most conservative of either instrument accuracy or instrument resolution. Perfect circles may not be the best assumption to describe the cross section of large exhaust ducts. This has been demonstrated by the distribution of chord lengths about the rotational positions shown in Fig. 12 and 13 of the Appendix.

2.2.3. Effective Mass Flow The computation of heat release rate by oxygen consumption, Eq. 1, requires a measurement of total mass flow in the exhaust duct. Measurements at the averaging pitot probes are used to compute mass flow through the exhaust ducts. Mass flow at each probe is computed as follows:

$$\dot{m}_{e,i} = \rho_{e,i} V_{e,i} \frac{\pi D_{eff}^2}{4} \tag{7}$$

The effective mass flow at the measurement station is the average measurement for the two probes, A and B:

$$\dot{m}_{eff} = (\dot{m}_{e,A} + \dot{m}_{e,B})/2 \tag{8}$$

A single averaging pitot probe (A) and thermocouple pair are installed vertically in the 0.483 m duct for the 0.5 MW calorimeter, hence $\dot{m}_{eff} = \dot{m}_{e,A}$.

Table 3
Effective Diameter of the Exhaust Ducts

Calorimeter	No. chord measurements	Effective duct diameter, m
0.5 MW	4	0.483 ± 0.004
3 MW, 10 MW	16	1.975 ± 0.005
20 MW	16	2.424 ± 0.009

2.2.4. Flow Measurement Uncertainty An uncertainty analysis was performed to estimate the combined uncertainty of the mass flow through the exhaust ducts as measured by the averaging pitot probes. The analysis uses the approximate methods described in the ISO GUM [24]. Assuming the input measurements were mutually independent, the following equation was applied to estimate the combined relative standard uncertainty:

$$\frac{u_c(y)}{y} = \sqrt{\sum_{i=1}^{N}\left(s_i\frac{u(x_i)}{x_i}\right)^2} \tag{9}$$

The relative standard uncertainty, $u(x_i)/x_i$, for each input measurement, x_i, used to compute mass flow, $y = \dot{m}_{\mathrm{eff}}$, is listed in Table 4. The non-dimensional sensitivity coefficient, given as,

$$s_i = \frac{\partial y}{\partial x_i}\frac{x_i}{y} \tag{10}$$

is also listed to reflect the weighting applied to the standard uncertainty of each component. The combined relative standard uncertainty is multiplied by a coverage factor of 2.0 to estimate the relative expanded uncertainty, $U(y)/y = 2.0\ u_c(y)/y$, with a confidence level of approximately 95%. Standard uncertainty estimates for the component measurements in Table 4 represent the accuracy and repeatability of the response of each instrument for a well-controlled and constant input.

Table 4 demonstrates the budget used to estimate the expanded uncertainty for mass flow derived from two averaging pitot probe measurements of gas velocity through the exhaust ducts. This estimate is approximately 3% for all conditions investigated. The estimate includes the potential contribution for measurement error due to a skewed velocity distribution, ε. This error has the potential to contribute more than 85% to the total uncertainty. Recall the flow coefficient, K_a, for the averaging pitot probe assumes an installation in a fully-developed turbulent pipe flow that is symmetric in all directions. When installed in less than ideal conditions, the potential for measurement error exists and will be discussed in later sections. The relative uncertainty due to this error is derived from the difference between mean flow measurements at probe A and probe B.

Table 4
Uncertainty Budget for the Mass Flow Through the Exhaust Duct as Measured by the Averaging Pitot Probes Servicing the 3 MW Calorimeter

Measurement/parameter, x_i (Units)	Value	$u(x_i)/x_i$	s_i	% Contribution
ε (−)	–	0.0144	1.0	88.8
K_a (−)	0.6271	0.0038	1.0	6.0
D_{eff} (m)	1.975	0.0013	2.0	2.7
R (J/kmol K)	8314.47	0.0000	− 0.5	0.0
M_{air} (kg/kmol)	28.97	0.0035	0.5	1.3
P_{amb} (Pa)	100,762	0.000 51	0.5	0.0
ΔP_A (Pa)	27.162	0.0030	0.25	0.2
ΔP_B (Pa)	25.442	0.0030	0.25	0.2
$T_{e,A1}$ (K)	396.8	0.0051	− 0.13	0.2
$T_{e,A2}$ (K)	396.6	0.0051	− 0.13	0.2
$T_{e,B1}$ (K)	395.4	0.0051	− 0.12	0.2
$T_{e,B2}$ (K)	395.3	0.0051	− 0.12	0.2
$\dot{m}_{e,A}$ (kg/s)	13.32	–	–	–
$\dot{m}_{e,B}$ (kg/s)	12.92	–	–	–
$\dot{m}_{eff}$ **(kg/s)**	**13.12**	$u_c/\dot{m}_{eff} = \mathbf{0.0153}$ $U/\dot{m}_{eff} = \mathbf{0.031}$		

$$\frac{u(\varepsilon)}{\varepsilon} = \frac{\bar{V}_{e,A} - \bar{V}_{e,B}}{\bar{V}_{eff} 2\sqrt{3}} \tag{11}$$

Whenever there are two or more averaging pitot probes installed on different chords, it is reasonable to assume that the actual mean velocity lies within the range of the measurements. If a rectangular distribution of possible mean values is further assumed, the uncertainty due to measurement error or measurement bias is described by Eq. 11. This follows a similar methodology developed to estimate measurement error from simulated flow distributions generated using computational fluid dynamics [22].

3. Results and Discussion

3.1. Flow Distribution and Flow Stability

A time history trace of the gas velocity measured at each of the averaging pitot probes in the 1.975 m exhaust duct is shown in Fig. 5. These measurements show that the gas velocity at Probe A is different than the gas velocity at Probe B, and hence it is possible for identical devices in the same flow stream to give different results. This is due to the devices being placed in different sectors of a skewed flow distribution and therefore being subject to different flow profiles across the length of the probes. Figure 5 also displays the ratio of the two gas velocity mea-

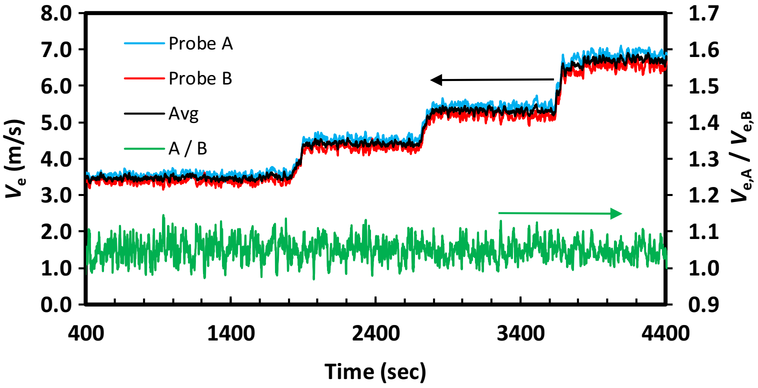

Figure 5. Time trace of gas velocity measurements from two averaging pitot probes mounted along orthogonal chords.

surements, $V_{e,A}/V_{e,B}$, which is slightly greater than unity and demonstrates the potential for measurement error when only one averaging pitot probe is used. Hence the average of the two measurements is used to define an effective gas velocity for the exhaust flow.

When two averaging pitot probes are installed along orthogonal chords, each probe interrogates a different portion of the flow and the two measurements offer some information about the symmetry of the flow. For example, assuming the upstream presence of probe A has a negligible impact on the flow measurement at probe B, a completely symmetric or ideal velocity distribution should give a ratio equal to 1.0, Fig. 6 (left-most diagram). Likewise, a velocity distribution that is skewed but with horizontal symmetry or vertical symmetry should give a ratio close to 1.0, Fig. 6 (center diagrams). A ratio other than 1.0 suggest that the velocity distribution is skewed and without symmetry on the horizontal and vertical centerlines, Fig. 6 (right-most diagram). A ratio other than one also suggest the potential for measurement error for each individual probe. In a study for a previous configuration of the exhaust ducts, point measurements of gas velocity were conducted to characterize the flow profiles along two orthogonal chords of the duct [22]. These measurements provided evidence of a skewed flow distribution with symmetry along a chord other than horizontal or vertical. Considering this evidence and the limits of budget and physical access, two averaging pitot probes were installed to improve the accuracy of the flow measurement.

Figure 7 displays the ratio with respect to Reynolds number, as defined by flow over the averaging pitot probe, for the full operational range of the 3 MW, 10 MW, and 20 MW calorimeters. The width of the averaging pitot probe is the characteristic dimension used to define Reynolds number, not the diameter of the duct. The 3 MW calorimeter is serviced by the 1.975 m exhaust duct. The average ratio of flow measured by the two averaging pitot probes is 1.050. This ratio suggests a skewed velocity distribution where horizontal or vertical symmetry does not occur. The difference in measurements from these two averaging pitot probes

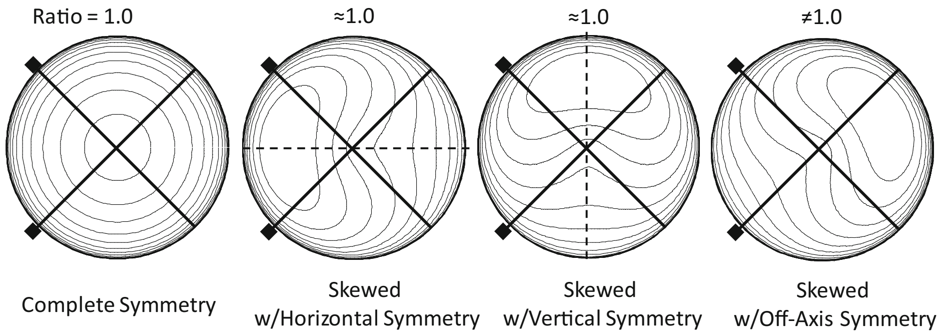

Figure 6. Illustrative examples of ideal and actual flow distributions and the anticipated ratio of flow measured by two averaging pitot probes mounted on orthogonal chords.

is the basis for estimating measurement error in Sect. 2.2. The standard deviation, σ, of the data is 0.008, indicating that the stability of the flow distribution is approximately 1.0%.

The 10 MW calorimeter is also serviced by the 1.975 m exhaust duct and shares the same averaging pitot probes as the 3 MW calorimeter, Fig. 3. The averaging pitot probes have an average flow ratio of 0.988 with a standard deviation of 0.009. This result is significant because the difference in the flow ratios for the two calorimeters is 0.062, which is much greater than the standard deviation of either ratio. The results of Fig. 7 are evidence that the flow ratio determined from a set of averaging pitot probes is useful to detect changes in velocity distribution. The 20 MW calorimeter, serviced by the 2.424 m exhaust duct, has an average flow ratio of 1.002 for the two averaging pitot probes, with a standard deviation of 0.009. This ratio is close to unity and suggest near vertical or horizontal symmetry in the velocity distribution. Vertical symmetry, as shown in Fig. 6, is consistent with the 90 vertical bend located upstream of the straight section in the 2.424 m exhaust duct, Fig. 3.

A minimum of three repeat experiments were conducted at each condition, ambient or heated flow; meaning at least six experiments were conducted at each calorimeter to generate the results of Fig. 7. As seen in Table 5, the standard deviation of the mean flow ratio is approximately 0.01 or less for all cases. This indicates that the flow distribution in each calorimeter is anticipated to remain stable to within 1.0% over the operational range of the calorimeter. A larger variation in the flow ratio occurs whenever the flow over the averaging pitot probe is below the recommended lower limit for Reynolds number, 12,500. This is apparent for the 3 MW and 10 MW calorimeters, and especially the case of heated flows at the 3 MW calorimeter. The flow ratio between two averaging pitot probes is a good quality control parameter for any duct flow measurement; it serves as an alert to significant changes in flow, to degraded performance at either of the devices due to clogging or excessive flow deposits, or to malfunctioning of either pressure transducer.

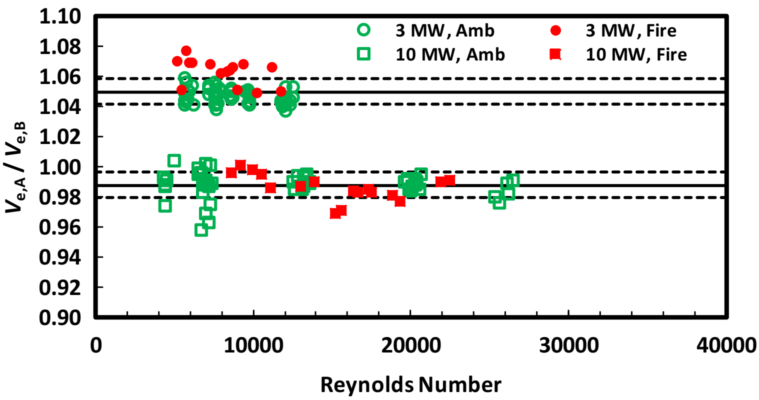

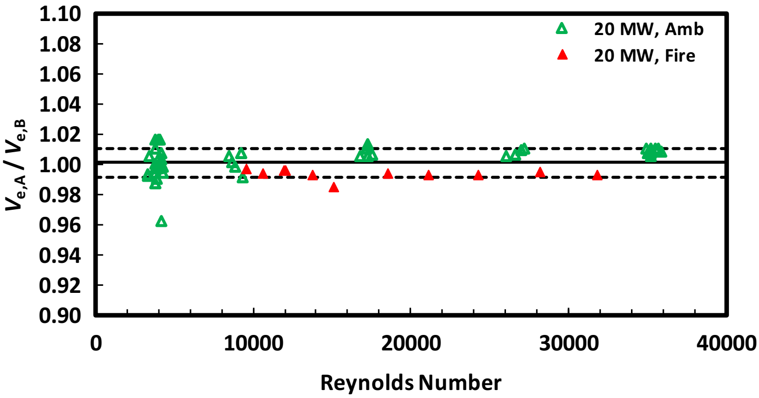

Figure 7. **Ratio of gas velocity determined from the two averaging pitot probes for the flow paths servicing the 3 MW (1.975 m duct), 10 MW (1.975 m duct), and 20 MW calorimeters. Solid lines and dashed lines represent mean and one standard deviation, respectively.**

Table 5
Statistics for the Ratio of Gas Velocity Determined for the Two Averaging Pitot Probes INSTALLED in the 3 MW, 10 MW, and 20 MW Calorimeters

	Flow ratio (mean ± σ)		
Calorimeter, Duct ID	Ambient	Heated	All Conditions
3 MW, 1.975 m	1.047 ± 0.005	1.063 ± 0.009	1.050 ± 0.008
10 MW, 1.975 m	0.988 ± 0.009	0.987 ± 0.009	0.988 ± 0.009
20 MW, 2.424 m	1.003 ± 0.009	0.994 ± 0.003	1.002 ± 0.009

More than 10 diameters of straight run exist upstream of each flow measurement location to allow for well-developed flow at the measurement station. Flow conditioning, such as screens, straightening tubes, or disturbance plates, has not been implemented. The results show that the ratio of the velocity, $V_{e,A}/V_{e,B}$ deviated from unity for some flow cases, suggesting skewed flow distributions. Therefore, in-line calibrations of the probes are recommended to improve measurement accuracy whenever the accuracy requirements of the desired measurement exceed what can be achieved with the probes alone.

3.2. Heat Release Rate Confirmation

Consensus standards for large fire calorimetry usually state that the flow measurement should be calibrated. A few of the standards (ASTM E2067, ISO 9705, NFPA 265) provide a limited description of the method to calibrate the flow measurement separate from the rest of the system. Alternatively, the standards address this need for flow calibration with a system calibration for the oxygen consumption calorimetry measurement using a gas burner with propane or methane as the fuel. This is essentially a method to determine the flow correction or flow shape factor. Within this description, limits for the difference between oxygen consumption calorimetry measurements and burner theoretical heat output are defined. These limits are usually equal to or greater than the required accuracy of the flow measurement. Table 6 lists the maximum allowable difference for some of the relevant standards. An allowable difference of 5% is typical, however a 10% difference is allowed for ISO 24473 which provides guidance on studying fires up to 40 MW. ASTM E2257 allows a 20% difference but requires that a calibration constant is calculated from the difference and used for future measurements. The standards state that whenever the limits are exceeded, the operator must determine the cause of the discrepancy, correct it, and re-calibrate the system.

A series of confirmation experiments were conducted to compare the rate of heat release derived from oxygen consumption (OC) calorimetry measurements, $\dot{Q}_{\mathrm{OC}}$, and the theoretical heat output from natural gas burners. An example of the time history data is displayed in Fig. 8. Five steps of steady heat output were generated at the natural gas burner. The steady period was maintained for a minimum of 3 min and data were recorded once every second. Theoretical heat output at the gas burner, or heat release rate by fuel consumption (FC) calorimetry, $\dot{Q}_{\mathrm{FC}}$, was computed from continuous measurements of the flow and heat content of natural gas. Detailed descriptions of NFRL's oxygen consumption and fuel consumption calorimetry measurements are described in a previous publication by the authors [21]. The results presented here for oxygen consumption calorimetry are prior to calibrating the exhaust flow measurements. These confirmation experiments are routine procedure. They are used to generate the full range of heat release anticipated for a fire test and exercise all components of the oxygen consumption calorimetry measurement. This procedure provides a convenient check that all instrumentation in the calorimetry system is operating at anticipated performance.

Table 6
System Calibration Requirements for Large Fire Calorimetry

Consensus standard	Flow measurement accuracy	Maximum burner output, MW	Maximum allowable difference
ASTM E2067	6%*	0.16	5%
ASTM E2257	–	0.30	20%
ISO 9705	5%	0.30	5%
ISO 24473	5%	0.30#	10%
NFPA 265	–	0.15	5%
NFPA 286	–	0.16	5%

*Most restrictive of the two values listed
#or 30% of the range of HRR for which the data are to be used

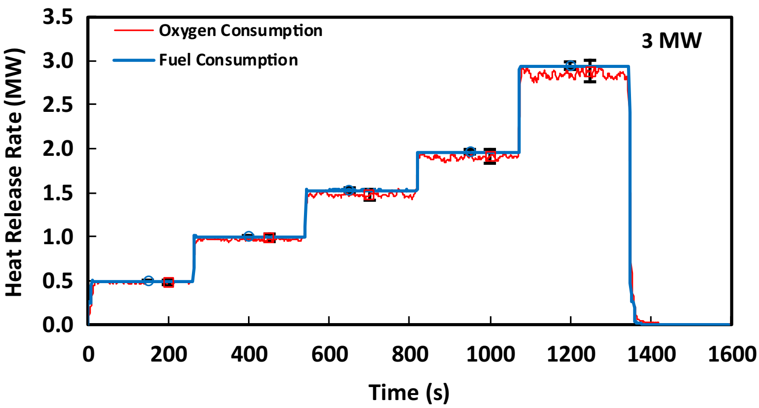

Figure 8. Time history trace of calorimetry confirmation experiments at the 3 MW calorimeter. A natural gas burner was used to generate the prescribed fires. Error bars represent expanded uncertainty.

NFRL's natural gas burners are part of a high precision fuel consumption calorimetry system. Theoretical heat output from each burner has an expanded measurement uncertainty of less than 2% [21]. The relative difference between mean values of heat release rate measured by oxygen consumption calorimetry and mean values of the theoretical heat output, $\bar{\dot{Q}}_{\mathrm{OC}}/\bar{\dot{Q}}_{\mathrm{FC}} - 1.0$, are plotted in Figs. 9 and 10. The heat output ranged from 0.1 MW to 20 MW and exhaust flows ranged from 50% to 100% of full scale, covering the range of routine operating conditions for the facility. The relative difference is less than 10% for all four calorimeters; meeting the system performance requirement for ISO 24473. The relative difference is less than 5% for the 0.5 MW, 3 MW, and 20 MW calorimeters; meeting the system performance requirements defined by most of the relevant standards.

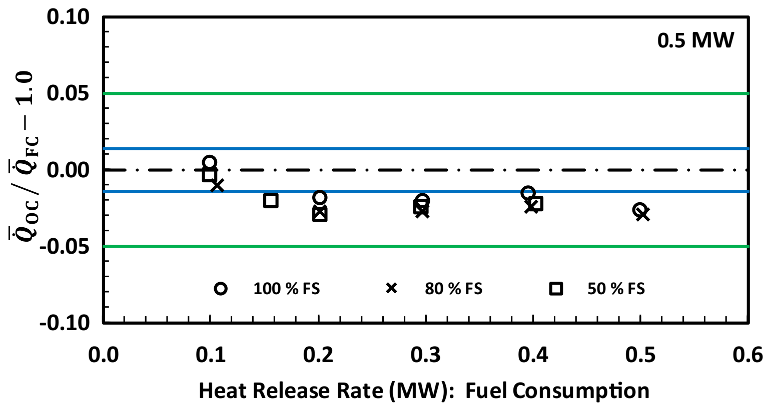

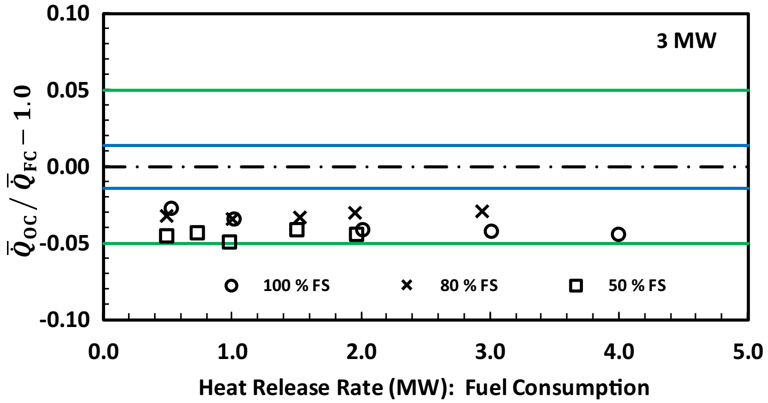

Figure 9. Results of the confirmation experiments for the 0.5 MW and 3 MW calorimeters. Dashed line: perfect agreement; Blue lines: expanded uncertainty of theoretical heat output from gas burner; Green lines: allowable maximum difference (most restrictive from Table 6); Symbols: exhaust flow, percent of full-scale (FS).

The results demonstrate that when two averaging pitot probes are installed along orthogonal chords, they are capable of meeting stated accuracy requirements without the need for an in-line (in situ) calibration. If the measurement of only one averaging pitot probe is utilized, the measurements still meet stated accuracy requirements. The largest velocity ratio, 1.05, occurs at the 3 MW calorimeter. Based on Eq. 3, the exhaust velocity at probe A is 2.4% greater than V_{eff} and the velocity a probe B is 2.4% lower than V_{eff}. Therefore, using a single averaging pitot probe measurement at the 3 MW calorimeter will result in a ± 2.4% shift in the data shown in Fig. 9 and still meet accuracy requirements. Since the velocity ratio is closer to unity for the 10 MW and 20 MW calorimeters, smaller shifts in the data shown in Fig. 10 will occur,. It is worth noting that the 0.5 MW calorimeter utilizes only one averaging pitot probe and still meets this require-

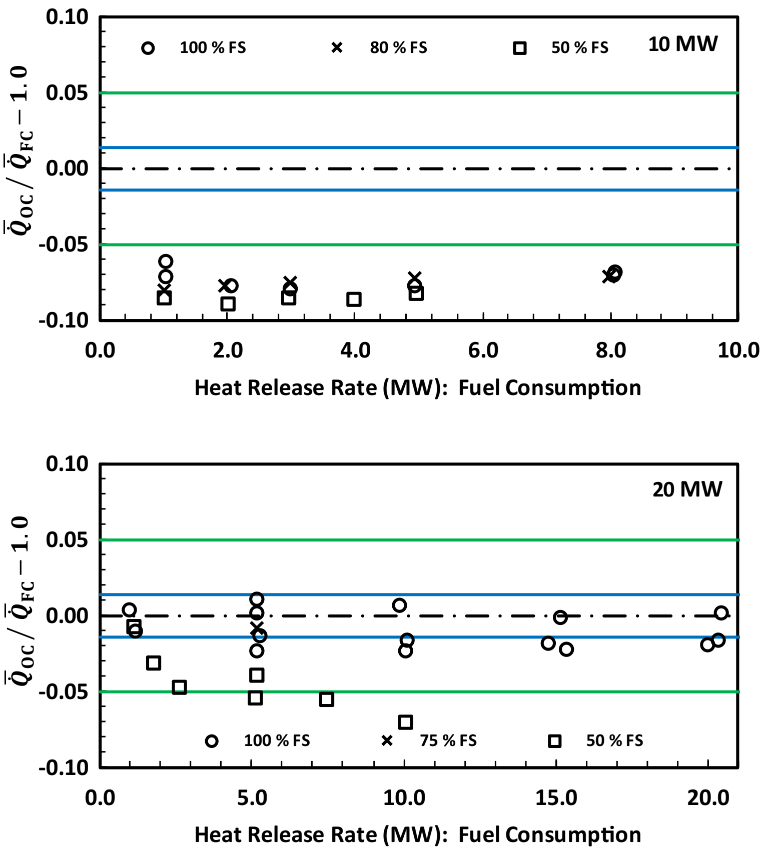

Figure 10. Results of the confirmation experiments for the 10 MW and 20 MW calorimeters. Dashed line: perfect agreement; Blue lines: expanded uncertainty of theoretical heat output from gas burner; Green lines: allowable maximum difference (most restrictive from Table 6); Symbols: exhaust flow, percent of full-scale (FS).

ment. This may be due to the high velocity (high Reynolds number) flow induced by the small diameter duct or simply due to a fortuitous placement of the probe. More data would be required to confirm either case. When budget and space allow, at least two averaging pitot probes are recommended, however one probe may be sufficient.

It is also worth noting that the performance of the averaging pitot probe has been demonstrated for fires up to 20 MW, which is almost 2 orders of magnitude greater than the largest heat output required by the standards during the system calibration. ASTM E2067 and ISO 24473 acknowledge that using higher burner outputs during the system calibration will improve accuracy [8, 9]. For laboratories with natural gas service from their local utility, demonstrating their performance over the full operational range of their calorimeter should be considered as a reasonable best practice.

4. Conclusions

Multiple studies have identified exhaust flow measurements as a significant source of uncertainty for large-scale calorimetry measurements. Further evidence of this can be inferred from the requirement to calibrate the heat release rate measurement against a known heat output that is almost universal among consensus standards for large fire testing. Averaging pitot probes are off-the-shelf technology that is widely used to monitor industrial process flows. They have been demonstrated here as the routine flow measurement device for a large fire calorimetry system. Their utilization has demonstrated that differences of less than 5%, between oxygen consumption calorimetry measurements and the theoretical heat output from gas burners, are possible. This meets the system performance requirements defined by the most relevant standards and provides evidence that repeat calibrations to meet accuracy requirements may not be necessary when averaging pitot probes are installed. However, this does not eliminate the need to use a known heat output to periodically confirm that all instruments in a large fire calorimeter are performing as anticipated. Whenever budget and space allow, at least two averaging pitot probes should be considered, but a single well-placed probe may also meet system accuracy requirements. The performance of the averaging pitot probe has been demonstrated for fires up to 20 MW, which is almost 2 orders of magnitude greater than the largest heat output required by the standards during the system calibration.

By design, averaging pitot probes integrate the velocity distribution in large exhaust ducts to provide a single measurement representative of the average flow. Depending on the accuracy requirements for a given test method or facility, they have the potential to reduce the need to apply corrections to heat release rate measurements in large fire testing. Averaging pitot probes are an affordable and practical means to monitor exhaust flows. Including this technology as an alternate method to measure exhaust flow should be considered as an improvement to relevant fire testing standards and to the overall accuracy of calorimetry measurements for large fire testing.

Acknowledgements

The authors are grateful to several members of the NFRL staff for their valuable contributions to this work: Laurean DeLauter and Anthony Chakalis, for installation of the averaging pitot probes; Marco Fernandez, for operations and data collection during confirmation experiments; Brian Story, for scale drawings of the exhaust system; and Christopher Smith, for assisting with the uncertainty analysis for the effective diameter measurement of the exhaust ducts.

Appendix: Accurate Determination Exhaust Duct Diameter

Accurate determination of the diameter of each exhaust duct is required to determine accurate measurements for volume flow, mass flow and ultimately heat release. The duct diameter is a squared term in the computation of volume or mass flow. Significant error for duct diameter measurements will propagate as a significant increase in flow measurement uncertainty. For example, 0.5% error in the duct measurement will propagate to become 1.0% error in the computation of cross-sectional area, which is used to compute volume or mass flow. Measurements of chord length were conducted at the locations of the averaging pitot probes and at various inclinations

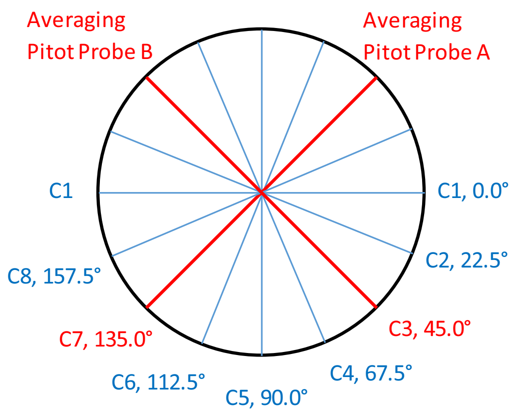

Figure 11. Locations of chord measurements at measurement locations as seen looking upstream and into the flow.

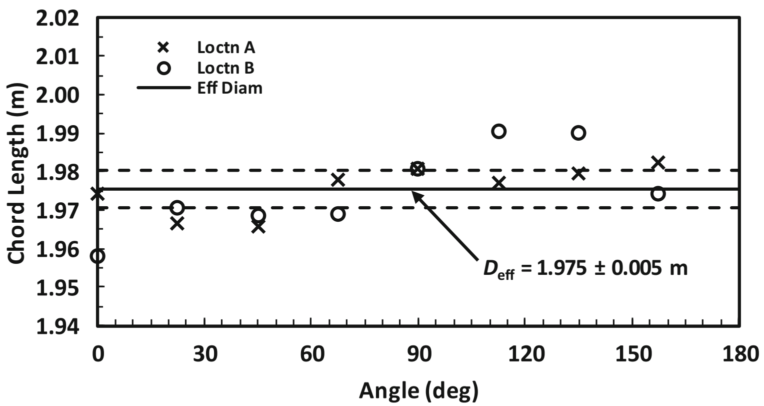

Figure 12. Distribution of chord lengths at the measurement stations of the averaging pitot probes for the 3 MW and the 10 MW calorimeters.

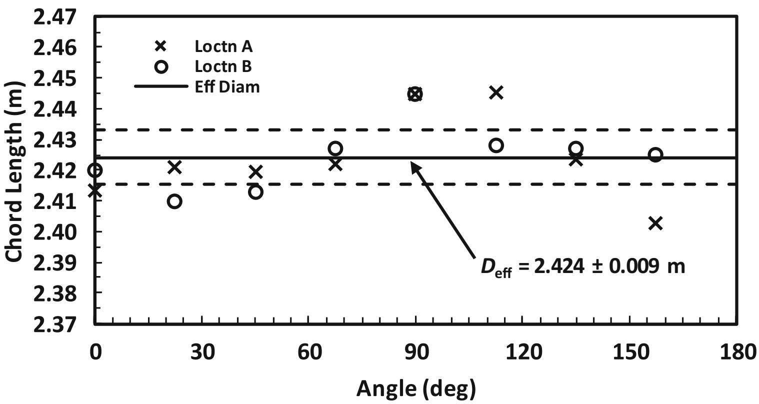

Figure 13. Distribution of chord lengths at the measurement stations of the averaging pitot probes for the 20 MW calorimeter.

to generate an accurate profile of the duct geometry. Using a laser distance meter (Leica DISTO D8) and a digital inclinometer, radial points were projected and marked on the inside surface of the exhaust ducts at increments of 22.5°, Fig. 11.

The distribution of chord lengths about the rotational positions, Figs. 12 and 13, confirms that the large ducts are not perfect circles. Therefore, the error in measurement could be substantial if only one chordal measurement were used to represent duct diameter.

References

1. Janssens ML (2002) Calorimetry. In: DiNenno PD, Beyler CL, Walton WD, Custer RLP, Hall JR, Watts JM (eds) The SFPE handbook of fire protection engineering, Chapter 2, 3rd edn, Section 3. National Fire Protection Association, Quincy, pp 38–62
2. Yeager RW (1986) Uncertainty analysis of energy-release rate measurement for room fires. J Fire Sci 4(4):276–296
3. Enright PA, Fleischmann CM (1999) Uncertainty of heat release rate calculation of the ISO5660-1 cone calorimeter standard test method. Fire Technol 35(2):153–169
4. Axelsson J, Andersson P, Lonnermark A, VanHees P, Wetterlund I (2001) Uncertainties in measuring heat and smoke release rates in the room/corner test and the SBI (Boras, Sweden). SP Report 2001:04, 2001
5. Brohez S (2005) Uncertainty analysis of heat release rate measurement from oxygen consumption calorimetry. Fire Mater 29(6):383–394
6. Sette B (2005) Evaluation of uncertainty and improvement of the single burning item test method. Ph.D. Thesis, University of Ghent, Belgium
7. Bryant RA, Mulholland GW (2008) A guide to characterizing heat release rate measurement uncertainty for full-scale fire tests. Fire Mater 32(3):121–139. https://doi.org/10.1002/fam.959
8. ASTM (2015) Standard practice for full-scale oxygen consumption calorimetry fire tests. ASTM International, West Conshohocken, PA, ASTM E 2067-15

9. ISO (2008) Fire tests - open calorimetry-measurement of the rate of production of heat and combustion products for fires of up to 40 MW. International Organization for Standardization, Switzerland, ISO 24473:2008(E)
10. ASTM (2017) Standard test method for room fire test of wall and ceiling materials and assemblies. ASTM International, West Conshohocken, PA, ASTM E 2257-17
11. ISO (1993) Fire tests-full-scale room test for surface products. International Organization for Standardization, Switzerland, ISO 9705:1993(E)
12. ASTM (2016) Standard test method for heat and visible smoke release rates for materials and products using an oxygen consumption calorimeter. ASTM International, West Conshohocken, PA, ASTM E 1354-16a
13. NFPA (2019) Fire tests for evaluating room fire growth contribution of textile or expanded vinyl wall coverings on full height panels and walls. National Fire Protection Association, Quincy, MA, NFPA 265
14. NFPA (2019) Fire tests for evaluating contribution of wall and ceiling interior finish to room fire growth. National Fire Protection Association, Quincy, MA, NFPA 286
15. Taylor JC (1987) Flow measurement by self-averaging pitot-tubes. Meas Control 20(10):145–147. https://doi.org/10.1177/002029408702001003
16. Kabacinski M, Pospolita J (2011) Experimental research into a new design of flow-averaging tube. Flow Meas Instrum 22(5):421–427. https://doi.org/10.1016/j.flowmeasinst.2011.06.006
17. Zhang JL, Li W, Liang RB, Zhao TY, Liu YC, Liu MS (2017) Numerical and experimental research on pentagonal cross-section of the averaging Pitot tube. Meas Sci Technol . https://doi.org/10.1088/1361-6501/aa6a04
18. Dobrowolski B, Kabacinski M, Pospolita J (2005) A mathematical model of the self-averaging Pitot tube—a mathematical model of a flow sensor. Flow Meas Instrum 16(4):251–265. https://doi.org/10.1016/j.flowmeasinst.2005.02.001
19. Wecel D, Chmielniak T, Kotowicz J (2008) Experimental and numerical investigations of the averaging Pitot tube and analysis of installation effects on the flow coefficient. Flow Meas Instrum 19(5):301–306. https://doi.org/10.1016/j.flowmeasinst.2008.03.002
20. Bundy M, Hamins A, Gross J, Grosshandler W, Choe L (2016) Structural fire experimental capabilities at the NIST National Fire Research Laboratory. Fire Technol 52(4):959–966. https://doi.org/10.1007/s10694-015-0544-4
21. Bryant RA, Bundy MF (2019). The NIST 20 MW calorimetry measurement system for large-fire research. National Institute of Standards and Technology, Gaithersburg, MD. https://doi.org/10.6028/NIST.TN.2077
22. Bryant R, Sanni O, Moore E, Bundy M, Johnson A (2014) An uncertainty analysis of mean flow velocity measurements used to quantify emissions from stationary sources. J Air Waste Manag Assoc 64(6):679–689. https://doi.org/10.1080/10962247.2014.881437
23. Rosemount (2006) Rosemount 485 annubar flow handbook. Rosemount Incorporated, Chanhassen, MN., Reference Manual 00809-0100-1191, RevCB
24. ISO (2008) Evaluation of measurement data - guide to the expression of uncertainty in measurement. International Organization for Standardization, Switzerland, JCGM 100:2008

Publisher's Note Springer Nature remains neutral with regard to jurisdictional claims in published maps and institutional affiliations.